EFFECT OF COOLING RATE FROM SOLUTION TREATMENT ON PRECIPITATION BEHAVIOR AND MECHANICAL PROPERTIES OF ALLOY 706

Takashi Shibata*, Tatsuya Takahashi*, Yukoh Shudo*, Mikio Kusuhashi*,
Jun-ichi Taira**, and Tohru Ishiguro**

Muroran Research Laboratory*, Muroran Plant**
The Japan Steel Works, LTD.
4 Chatsu-machi, Muroran, Hokkaido, 051 Japan

Abstract

The time - temperature - precipitation behavior of Ni-Fe-base superalloy 706 is very complicated because many kinds of precipitates exist in this alloy. Therefore, TTP behavior of this alloy vary with the heat treatment program and condition, and so do mechanical properties accordingly. In this study, TTP and TTH diagrams on cooling from the solution treatment of three experimental alloys and Alloy 706 are presented in a temperature range from 600 to 900℃ for up to 100h. The observations by optical microscopy, scanning electron microscopy and transmission electron microscopy revealed that γ', γ'', double cuboidal γ'-γ'' co-precipitate (compact morphology), overlaid γ'-γ'' co-precipitate (non-compact morphology) and η appeared in this alloy despite that the double cuboidal co-precipitate does not exist in the usual TTP diagram which is composed on re-heating from room temperature after the solution treatment.

The dependence of microstructure and mechanical properties of aged Alloy 706 on the cooling rate after the solution treatment was also examined. The solution treatment was conducted at 980℃ for 3h, and the cooling rate was varied from 0.5 to 85 ℃/min. Tensile strength and 0.2% yield strength were maximized at 3~5 ℃/min, while elongation and reduction of area suddenly decreased below 3~5 ℃/min. Creep rupture life was also maximized at 3~5 ℃/min, but creep rupture ductility suddenly increased below 3~5 ℃/min. These changes can be explained in terms of the precipitation behavior such as the formation of η at grain boundaries and the double cuboidal γ'-γ'' co-precipitate inside grains in the case of low cooling rate.

Superalloys 718, 625, 706 and Various Derivatives
Edited by E.A. Loria
The Minerals, Metals & Materials Society, 1997

Introduction

Ni-Fe-base superalloys are age-hardened by the precipitation of coherent γ' and/or γ'' in the austenitic matrix γ (1). Alloy 706 is a relatively new material and was developed from Alloy 718, a representative wrought superalloy. Compared with Alloy 718, Alloy 706 has a chemical composition of no molybdenum, reduced niobium, aluminum, chromium, nickel and carbon, and increased titanium and iron. This excellent balance of these allloying elements results in superior characteristics to Alloy 718 in segregation tendency, hot workability and machinability (2-4). Therefore, Alloy 706 is suitable for large forgings and has been used for high temperature services (5).

The time - temperature - precipitation (TTP) diagram is one of essential tools for designing the heat treatment for precipitation strengthened superalloy. Especially for Alloy 706, TTP behavior is very important because many kinds of precipitates exist in this alloy, and its mechanical properties are greatly affected by the precipitation at the heat treatment (6-11). From this point of view, the TTP diagrams of Alloy 706 have already been presented (2,3,12), and recently we presented more updated one (13). That TTP diagram indicates that four types of precipitates, that is γ', γ'', overlaid γ'-γ'' co-precipitate (so called, "non-compact morphology") and η , appear in Alloy 706. However, double cuboidal γ'-γ'' co-precipitate (so called, "compact morphology"), which is known to be formed in Alloy 706 (11) under some specific heat treatment conditions, dose not appear.

In this study, the TTP and the time - temperature - hardness (TTH) diagrams on cooling from the solution treatment are presented for Alloy 706 and six experimental alloys, in order to examine the formation of double cuboidal γ'-γ'' co-precipitate. These types of TTP and TTH diagrams are named "on cooling TTP and TTH", and popular TTP and TTH diagrams composed on heating from room temperature after solution treatmet are named "on heating TTP and TTH". The second half of this paper deals with the change in the microstructure and mechanical properties of aged Alloy 706 with the cooling rates from the solution treatment, as a typical example of the application of "on cooling TTP" behavior to the production of large turbine disk forgings.

Procedure

Materials

Six heats of experimental alloys were melted in a 50 kg vacuum induction melting (VIM) furnace. The chemical composition of these six alloys are listed in Table I. Alloy 706 contains aluminum, titanium and niobium, but these experimental alloys contain only one or two of these elements. Nickel and chromium contents were nearly constant in all alloys as shown in Table I, with iron being the balance. All ingots were diffusion treated and subsequently forged to billets with a cross section of 30^{t} x 120^{w} mm^2. These billets were sectioned mechanically into samples of suitable sizes for the following experiments.

A commercial Alloy 706 was also used as a sample. The sample was taken from a large gas turbine disk manufactured from a vacuum induction melted (VIM) and electro slag remelted (ESR) ingot that was diffusion treated and subsequently forged. Its chemical composition is also given in Table I.

Table I Chemical Composition of Experimental Alloys

mass %

Heat	Ni	Fe	Cr	Al	Ti	Nb	C	N	O	B	Si	Mn	P	S
No.1	43.36	bal.	16.43	0.34	0.01	0.05	< 0.003	0.0033	0.0020	< 0.005	0.035	0.010	< 0.003	0.0008
No.2	43.75	bal.	16.23	0.04	1.68	0.05	0.003	0.0012	0.0025	< 0.005	0.035	0.010	< 0.003	0.0010
No.3	43.96	bal.	15.95	0.05	0.01	2.56	< 0.003	0.0043	0.0145	< 0.005	0.040	0.010	< 0.003	0.0009
No.4	43.54	bal.	16.29	0.30	1.71	0.05	< 0.003	0.0014	0.0018	< 0.005	0.025	0.010	< 0.003	0.0006
No.5	43.62	bal.	16.13	0.05	1.75	2.82	< 0.003	0.0026	0.0025	< 0.005	0.045	0.010	< 0.003	0.0009
No.6	43.76	bal.	16.30	0.30	0.01	2.54	0.003	0.0025	0.0010	< 0.005	0.050	0.010	< 0.003	0.0008
706	42.80	bal.	16.18	0.25	1.68	2.85	0.006	0.0041	0.0006	0.0048	0.020	0.020	< 0.003	0.0005

Heat Treatments

Heat treatment conditions for producing the "on cooling TTP" diagram are shown in Figure 1 (a). All of the samples were solution-treated at 980℃ for 3h. This condition was determined according to a previous report (13) so as to fully dissolve precipitates formed in the forging process and to obtain a mean grain size of ASTM #3-4. The heating

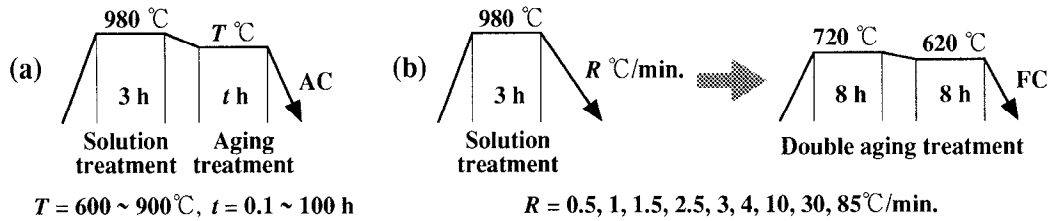

Figure 1 : Heat treatment programs and conditions.

rate to the solution treatment temperature was 50℃/h, simulating a practical large size forging. After the solution treatment, the samples were cooled down to various temperatures between 900 and 600℃ at 50℃/h and held isothermally up to 100h as shown in Figure 1 (a).

In order to clarify the effect of cooling rates from the solution treatment, Alloy 706 was heat - treated under the condition shown in Figure 1 (b). The solution treatment was conducted at 980℃ for 3h, and the cooling rate was varied from 0.5 to 85 ℃/min. This range of the cooling rate was chosen so as to simulate a various cooling methods of practical large size forging, such as furnace cooling, air cooling, oil quench and water quench. Subsequently they were double-aged at 720℃ for 8h and at 620℃ for 8h.

Evaluations of Precipitation Behavior

The heat treated samples were subjected to optical microscopy, scanning electron microscopy (SEM) and transmission electron microscopy (TEM) for their precipitation behavior. Thin film method was used for TEM sample preparation, and final thinning was achieved by electro-polishing. A 200kV TEM was used with micro-beam technique in both electron diffraction and energy dispersive X-ray spectroscopy (EDS), with the probe diameter being minimum 1nm. Hardness was measured by a Vickers hardness tester, in order to produce the "on cooling TTH" diagram.

Tests of Mechanical Properties

Tensile tests were performed at room temperature, on the samples aged after cooled at various cooling rates from the solution treatment. The diameter of specimens was 7mm and the gauge length was 35mm. Creep tests were also conducted at 650℃/ 686.5 MPa. The diameter of specimens was 6mm and the gauge length was 30mm. In order to ensure the uniformity of temperature, the specimens were held for 24h at the test temperatures before loading.

Results and Discussion

"On Cooling TTH" Diagram

Hardness of alloy No.1 changed little and hardness of alloys Nos. 3 and 6 changed a little after a long time exposure within the range of this experiment, indicating that either 0.3% aluminum or 2.5% niobium or the combination of both is insufficient for age hardening. It should be noted that alloys Nos. 3 and 6 were a little hardened in this study, that is in case of "on cooling TTH". On the contrary, alloys Nos. 3 and 6 were not hardened in case of usual "on heating TTH" (13). It suggests that the rate of formation of strengthening precipitate is higher in "on cooling TTP" than in "on heating TTP".

The titanium-free alloys were a little hardened by the heat treatment as described above, while titanium-containing alloys, namely Nos.2, 4, 5 and Alloy 706 were all age-hardenable, indicating the formation of γ ' and/or γ " phase. The "on cooling TTH" diagrams of three experimental alloys, Nos.2, 4 and 5, and Alloy 706 are shown in Figure 2. The highest hardness was about 400 Hv in No.5 and Alloy 706, but about 300 Hv in Nos.2 and 4. The higher hardness is attributed to niobium of those alloys, suggesting a synergetic effect between niobium and titanium. This is the same effect as "on heating TTH" diagram. On the contrary, the regions of highest hardness in "on cooling TTH" diagrams were different from those in "on heating TTH" diagram. The difference between them was especially distinct for the shorter time range at low temperature in TTH diagram. This difference is considered to be due to the precipitation of γ ' and/or γ " phase during the cooling stage from the solution treatment.

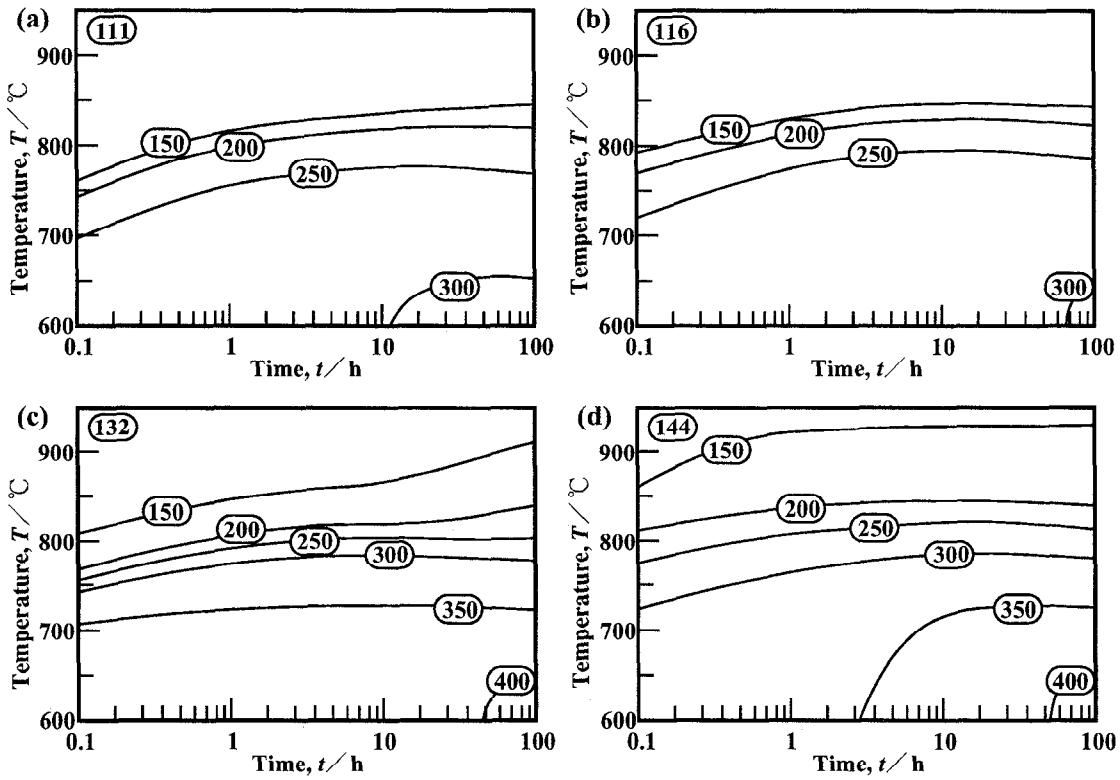

Figure 2 : The "on cooling TTH" diagrams of three experimental alloys and Alloy 706 : (a) alloy No.2, (b) No.4, (c) No.5 and (d) Alloy 706.

Identification of Precipitation

Five types of precipitates were identified in the alloys Nos. 2, 4, 5 and Alloy 706 by micro-beam electron diffraction and micro-beam EDS. They were γ ' phase, γ " phase, overlaid γ '- γ " co-precipitate, double cuboidal γ '- γ " co-precipitate and η phase. Typical TEM micrographs of these five precipitates are shown in Figure 3 (a) ~ (e).

The γ ' phase appeared in the alloys Nos. 2, 4 and Alloy 706. This precipitate had L_{12} structure (FCC like) and consisted of either nickel and titanium for alloy No. 2 or nickel, titanium and aluminum for alloy No. 4 or nickel, titanium, aluminum and niobium for Alloy 706. The γ " phase appeared in the alloy No. 5 and Alloy 706. This precipitates had DO_{22} structure (BCT like) and consisted of nickel, titanium and niobium. In all cases, the ratio of nickel to (titanium + niobium + aluminum) was nearly 3:1.

The overlaid γ '- γ " co-precipitate appeared in the alloy No.5 and Alloy 706. This co-preciptate had the core of γ ' phase being overlaid with the γ " phase on its top and/or bottom, which were referred to by R.Cozar and A.Pineau as "non-compact morphology" in the modified 718 alloys (14-23). The double cuboidal γ '- γ " co-precipitate appeared only in Alloy 706. This co-precipitates has the core of γ ' being completely covered with the γ " thin skin, referred to as co-precipitate of "compact morphlogy" (14-23). In both cases, the coherency between γ , γ ' and γ " is maintained. These two types of co-precipitates were also found in Alloy 706 stabilized and aged (11).

The η phase, having DO_{24} structure (HCP like), appeared in all alloys used in this study. The η phase consisted of nickel and titanium in alloys Nos.2 and 4, while it consisted of nickel, niobium and titanium in alloy No.5 and Alloy 706. However, the ratio of nickel to (titanium + niobium) was maintained nearly 3:1 in all alloys. The selected area diffraction pattern indicates that the η phase has a specific orientation relationship with the γ matrix, as $[011]_\gamma$ // $[2110]_\eta$ and $(111)_\eta$ // $(0001)_\gamma$. This is consistent with our previous work (11,13). The η phase appears parallel to each other in order to meet this orientation relationship. The η phase precipitation occured predominantly at the grain boundary, and it grew into the grain from the grain boundary as the exposure time increased.

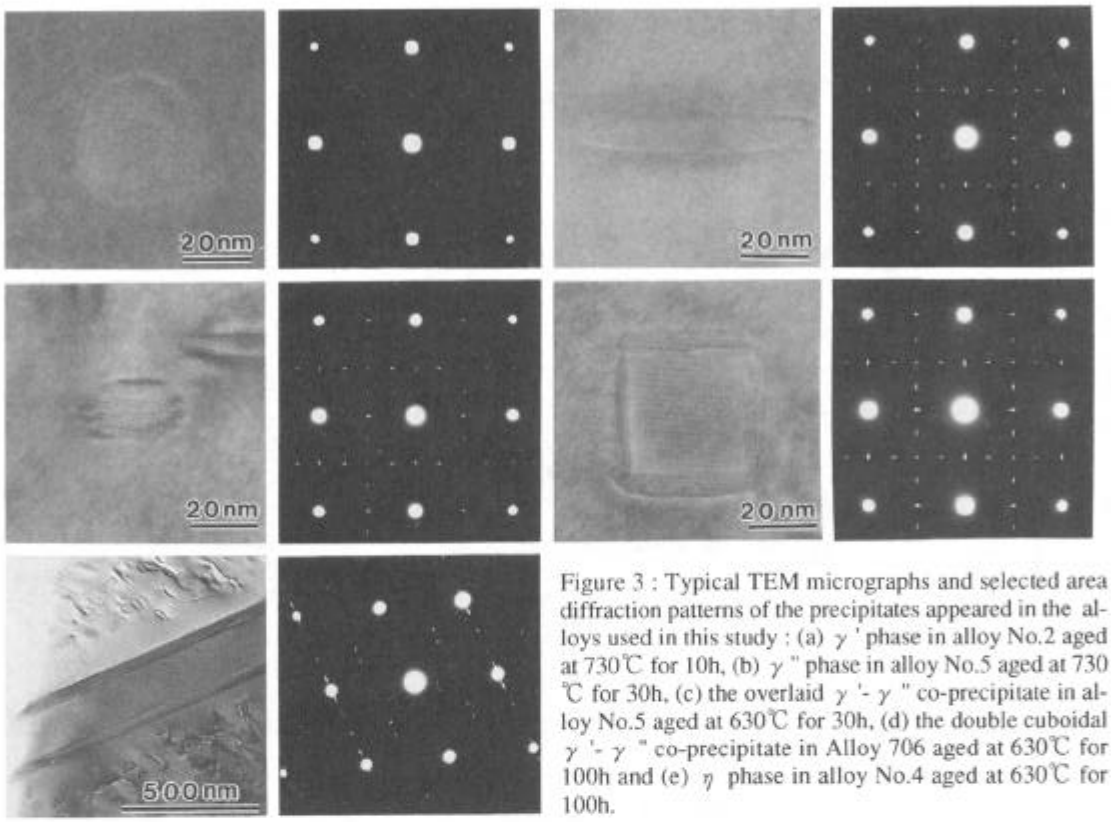

Figure 3 : Typical TEM micrographs and selected area diffraction patterns of the precipitates appeared in the alloys used in this study : (a) γ' phase in alloy No.2 aged at 730℃ for 10h, (b) γ'' phase in alloy No.5 aged at 730 ℃ for 30h, (c) the overlaid γ'- γ'' co-precipitate in alloy No.5 aged at 630℃ for 30h, (d) the double cuboidal γ'- γ'' co-precipitate in Alloy 706 aged at 630℃ for 100h and (e) η phase in alloy No.4 aged at 630℃ for 100h.

"On Cooling TTP" Diagram

The "on cooling TTP" diagrams of the four alloys, alloys Nos.2, 4, 5 and Alloy 706 are shown in Figure 4. The region of γ', γ'' and γ'- γ'' co-precipitates is agreed well with the TTH diagram. The "on cooling TTP" diagrams are consistent with the estimation from the "on heating TTP" diagrams. For the role of strengthening elements, which are titanium, niobium and aluminum, in TTP behavior, there is no substantial difference between the "on cooling TTP" behavior and the "on heating TTP" behavior (13). The only exception is the presence of the double cuboidal γ'- γ'' co-precipitate. This co-precipitate appears only in the "on cooling TTP" diagram of Alloy 706. The reason can be explained from the view of growth of γ' phase, in the following way.

The γ'- γ'' co-precipitate is considered to form through initial γ' formation and subsequent γ'' formation on that γ'. Therefore, in order to form co-precipitate, both γ' and γ'' are necessary. In fact, as compared alloy No.5 and Alloy 706 with alloys Nos. 2 and 4, this co-precipitate demands niobium that is a required element for the formation of γ'', in addition to titanium that can form γ'. However, only the overlaid co-precipitate appears in alloy No.5, while both the overlaid co-orecipitate and the double cuboidal co-orecipitate appear in Alloy 706. This seems to be due to the size of γ' before the formation of γ''. When that size is large enough to form γ'' on its six {100} planes, the double cuboidal co-precipitate can form (14). That is to say, in order to form double cuboidal co-precipitate, a relatively large γ' prior to the formation of γ'' is necessary. As compared Alloy 706 with alloy No.5, this co-precipitate demands aluminum that can only substitute in γ' and not in γ''. On the contrary, titanium can substitute both γ' and γ''. Therefore, aluminum promotes the formation γ' more than titanium does. In other words, this co-precipitate demands the co-existance of niobium for γ'' and aluminum for γ'. This tendency of the balance among aluminum, titanium and niobium is consisitent with the previous report on Alloy 718 (14-23).

The reason that this co-precipitate appears only in the "on cooling TTP" diagram is considered to be due to the difference in the rate of γ' formation. As shown in Figure 4, in case of "on cooling TTP", the precipitation of γ' occurs in upper side of γ'' region, whereas, in case of "on heating TTP", the precipitation of γ' occurs in lower side of γ'' region. Therefore, the temperature of γ' formation is higher in "on cooling TTP" than in "on heating TTP", so the rate of γ' formation is greater in "on cooling TTP" than in "on heating TTP". This high rate in the "on cooling TTP" is consistent with the estimation described in the "on cooling TTH" diagram of titanium-free alloys. As a result, the size of γ' is larger in "on cooling TTP" than in "on heating TTP".

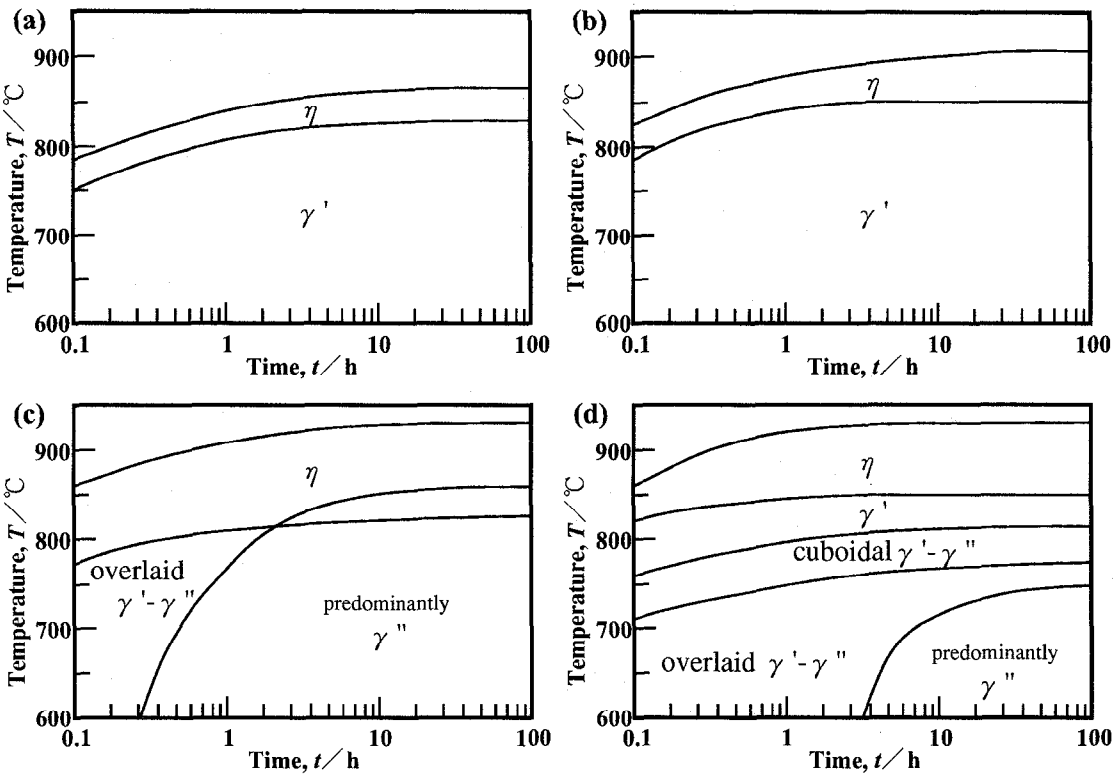

Figure 4 : The "on cooling TTP" diagrams of three experimental alloys and Alloy 706 : (a) alloy No.2, (b) No.4, (c) No.5 and (d) Alloy 706.

Tensile Tests of Aged Alloy 706 with Various Cooling Rates after Solution Treatment

Having obtained these results described above, the effect of the cooling rate after the solution treatment on the microstructure and mechanical properties of aged Alloy 706 were investigated in detail, as a typical example of the application of "on cooling TTP" behavior to the production of large turbine disk forgings.

The change in the tensile properties at room temperature with the cooling rate is shown in Figure 5. Tensile strength and 0.2% yield strength increased, as the cooling rate decreased down to 3℃/min. They were maximized at about 3 ℃/min and then decreased with the decreasing cooling rate. Elongation and reduction of area gradually decreased, as the cooling rate decreased down to 10℃/min. Then, they suddenly decreased below 5℃/min. These facts indicate that the tensile properties of Alloy 706 are greatly affected by the cooling rate after the solution treatment.

Creep Tests of Aged Alloy 706 with Various Cooling Rates after Solution Treatment

The changes in the creep rupture time, the creep elongation and the creep reduction of area with the cooling rate are shown in Figure 6. The creep rupture life increased, as the cooling rate decreased down to 3℃/min. It was maximized at about 3℃/min and then rapidly decreased with the decreasing cooling rate. Elongation and reduction of area gradually increased, as the cooling rate decreased down to 10℃/min. Then, they rapidly increased below 5℃/min. Therefore the creep properties of Alloy 706 are also greatly affected by the cooling rate from the solution treatment.

Change in Precipitation Behavior of Aged Alloy 706 with Various Cooling Rates after Solution Treatment

The above changes in tensile and creep properties suggest that the precipitation behavior in the cooling stage after the solution treatment, that is just the "on cooling TTP" behavior, has strong influence on the mechanical properties, even after the aging treatment. Therefore, in order to shed more light on the change in the precipitation behavior, SEM and TEM observations were conducted.

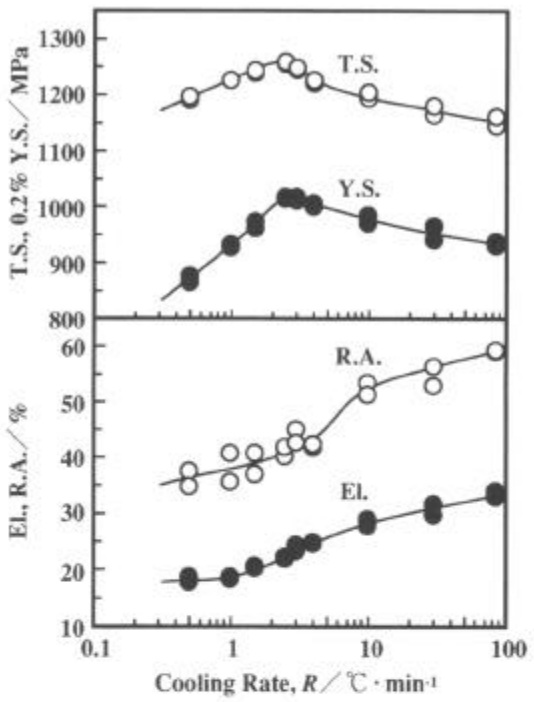

Figure 5 : Change in the tensile properties at room temperature of aged Alloy 706 with the cooling rate from the solution treatment.

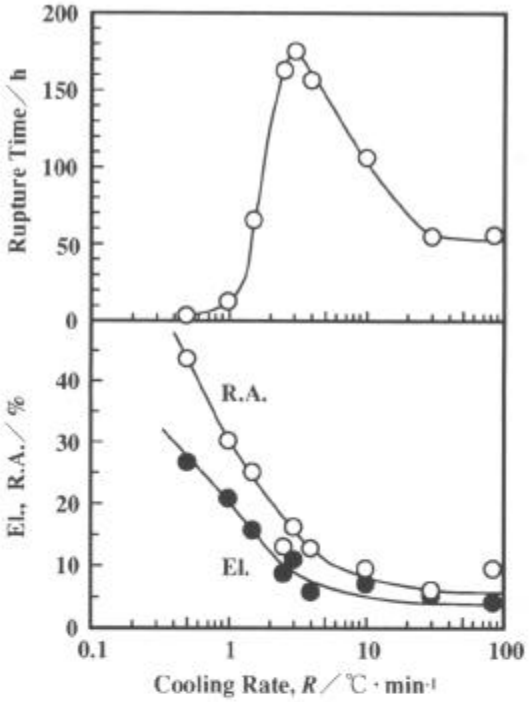

Figure 6 : Change in the creep rupture properties at 650℃/686 MPa of aged Alloy 706 with the cooling rate from the solution treatment.

The results obtained in this study has led to three groups of the cooling rate from solution treatment in terms of the precipitation behavior ; the high cooling rate above 10℃/min (Group A), the intermediate cooling rate from 10 to 2 ℃/min (Group B), and the low cooling rate below 2 ℃/min (Group C). Because of the limited pages, one representative observation for each group is presented here. Cooling rate of 85℃/min, 3℃/min and 0.5℃/min are adopted as the representative of Groups A, B and C, respectively.

Typical examples of SEM micrographs of aged Alloy 706 are shown Figure 7. No precipitate was observed at the grain boundary when the cooling rate was 85 ℃/min, while cellular precipitates were observed when the cooling rate were 3 and 0.5 ℃/min. These inter-granular precipitates existed in the all samples belonging to Groups B and C, and were more pronounced when the cooling rate was lower.

Figure 8 shows TEM micrographs at the grain boundary of aged Alloy 706 after cooled from the solution treatment temperature at rates of 3 and 0.5 ℃/min. The inter-granular precipitates in Figure 8 were identified as η phase by micro-beam diffraction and EDS. The composition and structure of the η phase were identical as those described in the TTP diagram. The specific orientation between η phase and the matrix was also the same. As shown in Figures 7 and 8, the precipitation of η resulted in the formation of the serrated grain boundary and denuded-zone around it. The denuded zone became wider and more distinct as the cooling rate decreased. In case of Group A, any precipitates were not observed at the grain boundary, even in the TEM scale. These facts on η phase are thought to be due to

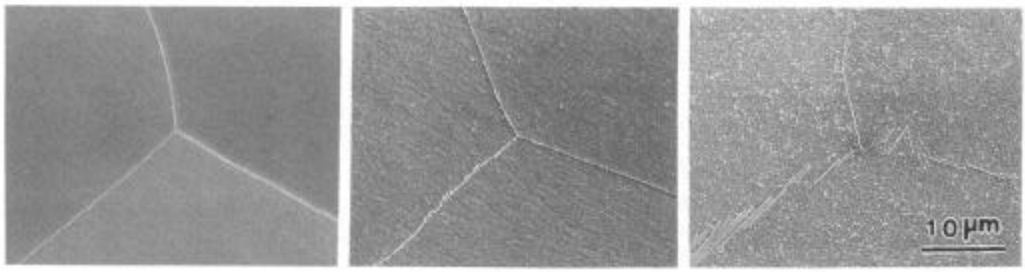

Figure 7 : SEM micrographs at the grain boundary of aged Alloy 706 after cooled from the solution treatment temperature at rates of (a) 85℃/min, (b) 3℃/min and (c) 0.5℃/min.

relatively low cooling rates in Group B, and are consistent with the prediction from the "on cooling TTP" and the phenomena of Alloy 706 stabilized and aged (11).

For the intra-ganular precipitates, four types of precipitates were identified in the aged Alloy 706. These were γ', γ'', double cuboidal γ'-γ'' co-precipitate, overlaid γ'-γ'' co-precipitate, which were the same kinds with the intra-granular precipitates appeared in the "on cooling TTP" digram of Alloy 706. The composition and structure of these four precipitates are the same as those described in the TTP diagram.

Figure 9 shows TEM micrographs inside a grain of aged Alloy 706 after cooled from the solution treatment temperature at rates of 85, 3 and 0.5 ℃/min. The overlaid co-precipitate and γ'' phase were observed in case of the cooling rate of 85℃/min. These precipitates were very fine and their size was below ten nanometers. The double cuboidal co-precipitates, their size being several ten nanometers, were observed in case of the cooling rate of 3 ℃/min, in addition to the fine overlaid co-precipitates. It is unclear which precipitate is dominant in case of Group B, at this moment. However, the double cuboidal co-precipitates were larger and more dominant, as the cooling rate became lower. When the cooling rate was as low as Group C, the large double cuboidal co-precipitates appeared predominantly. Their size was above 50 nanometers when the cooling rate was 0.5℃/min. The γ' phase was also observed in case of Group C, but rarely appeared. These observations are also consisitent with the prediction from the "on cooling TTP", especially in terms of the formation of γ' phase and the double cuboidal co-precipitate.

Relationship between the Precipitation Behavior and the Mechanical Properties

For Group A, the precipitation on the cooling stage from the solution treatment temperature is considered to hardly occur because of its high cooling rate. In fact, the hardening by precipitation seems to occur mainly in the aging treatment from Figure 10, showing the change in vickers hardness before and after the aging treatment with the cooling rate. The precipitation behavior of Group A is considered to virtually reflect the precipitation behavior in the aging treatment, hence its mechanical properties would be considered to directly reflect the condition of only aging treatment used in this study.

In the case of Group B, the precipitation on the cooling stage from the solution treatment can not be ignored, as estimated from Figure 10. Therefore its precipitation behavior changes from Group A's, so do mechanical properties accordingly. Tensile strength and 0.2% yield strength of Group B are higher than those of Group A, as seen in Figure 5. Group B's strengthening ability of the matrix is considerd to be greatest among these three groups, because of either the increase of total amount of

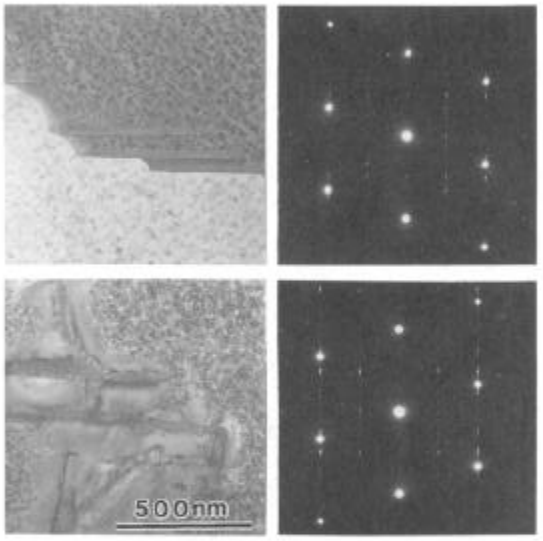

Figure 8 : TEM micrographs at the grain boundary of aged Alloy 706 after cooled from the solution treatment temperature at rates of (a) 3℃/min and (b) 0.5℃/min.

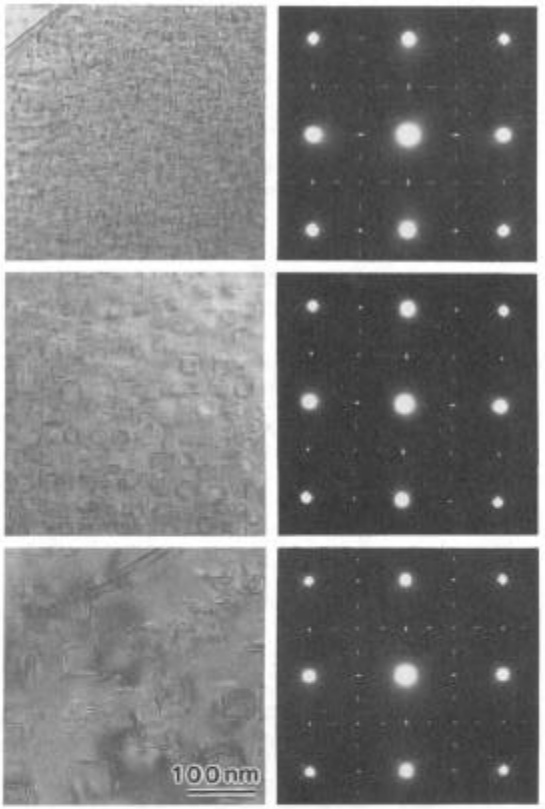

Figure 9 : TEM micrographsinside a grain of aged Alloy 706 after cooled from the solution treatment temperature at rates of (a) 85℃/min, (b) 3℃/min and (c) 0.5℃/min.

precipitates or the contribution of the co-existance of middle sized double cuboidal in addition to the fine overlaid co-precipitate. In order to understand this strengthening mechanism, a more precise study is needed.

Another characteristic difference in the precipitation behavior between Group A snd Group B is the η at the grain boundary, which results in the grain boundary serration and the denuded zone, as seen in Figures 7 and 8. These changes are the same as the stabilized and aged Alloy 706, and it has been reported that these changes near the grain boundary cause the degradation of tensile ductility and the improvement of creep properties (10,11). These are mainly due to the pinning of grain boundary by the η , grain boundary serration, and indistinct denuded zone. In fact, Figures 5 and 6 indicate that the elongation and the reduction of area rapidly decrease and that the creep properties are markedly improved, in accordance with the occurence of η precipitation.

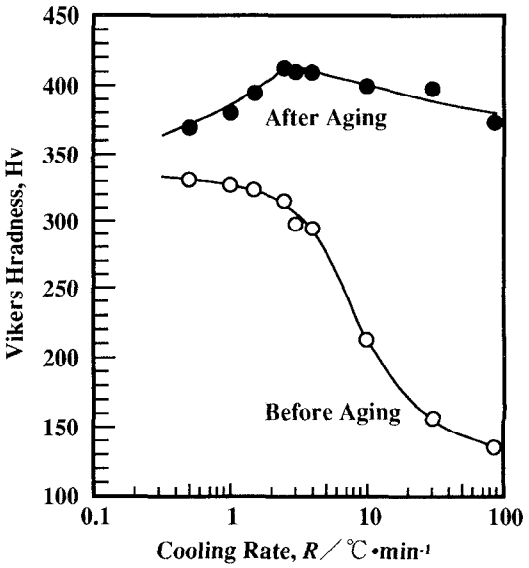

Figure 10 : Change in vickers hardness of Alloy 706 with the cooling rates from the solution treatment.

In the case of Group C, the difference in the hardness before and after the aging was very small as seen in Figure 10, indicating that the precipitation at the cooling stage from the solution treatment is predominant. In other words, the strengthening elements, titanium, niobium and aluminum, are mostly consumed for precipitation on the cooling stage from the solution treatment. Therefore, the large precipitates such as the γ ' phase and the double cuboidal co-precipitate are dominant as predicted from the "on cooling TTP" diagram. Indeed, these precipitates predominantly appeared in Group C, as seen in Figure 9 (c). At the same time, η phase grows larger and the denuded zone becomes wider, as seen in Figures 7 and 8. In general, the smaller the precipitates, the more effective they are in precipitation hardening and the thermally more stable they are (1). Therefore, the degradation of mechanical properties in Group C, as shown in Figures 5 and 6, is attributed to these coarsened precipitates in the grain matrix. The wide denuded zone around η is thought to readily cause grain boundary sliding at high temperatures whereby overshadowing the beneficial effect of η precipitation.

From the results of this study, the cooling rate should be strictly controlled so as to give preferable properties. Especially for the large forgings, the cooling rate is very different between the surface and the mid-thickness portion. Therefore, the prediction of the cooling rate at each location of the forgings is seriously important, and the cooling method should be selected so that the whole forgings is within a range of appropriate cooling rates.

As described above, the "on cooling TTP" behavior is consistent with the changes in the precipitation behavior on the cooling stage after solution treatment. Accodingly it can be applied to estimate the change in the mechanical properties. In the case of heat treatment of Alloy 706, "on heating TTP" and "on cooling TTP" can offer a variety of practically important imformation.

Conclusions

In order to clarify the precipitation behavior of Alloy 706, the "on cooling TTH" and "on cooling TTP" diagrams of Alloy 706 and three experimental alloys are presented. The precipitates appeared in these four alloys are identified to γ ' phase, γ " phase, overlaid γ '- γ " co-precipitate, double cuboidal γ '- γ " co-precipitate and η phase. In the case of Alloy 706, all of these five precipitates appear, being all of the important precipitates in this alloy. Especially, the double cuboidal co-precipitate appears only "on cooling TTP" diagram of Alloy 706. It would be due to the co-existance of aluminum, niobium and titanium and the heat sequence used in the "on cooling TTP".

The microstructure and mechanical properties of aged Alloy 706 were found to change considerably with the cooling rate after the solution tratment. Tensile strength and 0.2% yield strength are maximized at 3~5 ℃/min, but elongation and reduction of area suddenly decrease below 3~5 ℃/min. Creep rupture life is also maximized at 3~5 ℃/min, but creep rupture ductility suddenly increases below 3~5 ℃/min. These changes can be explained in terms of the changes in the precipitation behavior during the cooling stage from the solution treatment temperature such as the formation of η at grain boundary and the double cuboidal γ '- γ " co-precipitate inside a grain because of the low cooling rate, which are consistent with the prediction from the "on cooling TTP" diagram.

References

1. E.E.Brown and D.R.Muzyka, "Nickel-Iron Alloys", Superalloys II, ed., C.T.Sims, N.S.Stoloff, and W.C.Hagel (New York, John Willey & Sons, 1987), 165-188.
2. H.L.Eiselstein, "Properties of Inconel Alloy 706", ASM Technical Report, No.C 70-9.5 (1970), 1-21.
3. H.L.Eiselstein, "Properties of a Fabricable, High Strength Superalloy", Metals Engineering Quarterly, November (1971), 20-25.
4. E.L.Raymond and D.A.Wells, "Effects of Aluminum Content and Heat Treatment on Gamma Prime Structure and Yield Strength of Inconel Nickel-Chromium Alloy 706", Superalloys --Processing (Columbus, OH:Metals and Ceramics Information Center, 1972), N1-N21.
5. P.W.Schilke, J.J.Pepe, and R.C.Schwant, "Alloy 706 Metallurgy and Turbine Wheel Application", Superalloys 718,625,706 and Various Derivatives, ed., E.A.Loria (Warrendale, PA:TMS, 1994), 1-12.
6. J.H.Moll, G.N.Maniar, and D.R.Muzyka, "The Microstructure of 706, a New Fe-Ni-Base Superalloy", Metallurgi cal Transactions, 2(1971), 2143-2151.
7. J.H.Moll, G.N.Maniar, and D.R.Muzyka, "Heat Treatment of 706 Alloy for Optimum 1200 ° F Stress-Rupture Properties", Metallurgical Transactions, 2(1971), 2153-2160.
8. L.Remy, J.Laniesse, and H.Aubert, "Precipitation Behavior and Creep Rupture of 706 Type Alloys", Materials Science and Engineering, 38(1979), 227-239.
9. G.W.Kuhlman, A.K.Chakrabarti, R.A.Beaumont, E.D.Seaton, and J.F.Radavich, "Microstructure - Mechanical Properties Relationships in Inconel 706 Superalloy", Superalloys 718, 625, 706 and Various Derivatives, ed., E.A.Loria (Warrandale, PA:TMS, 1994), 441-449.
10. T.Takahashi, T.Ishiguro, K.Orita, J.Taira, T.Shibata, and S.Nakata, "Effects of Grain Boundary Precipitation on Creep Rupture Properties of Alloy 706 and 718 Turbine Disk Forgings", ibid., 557-565.
11. T.Shibata, Y.Shudo, T.Takahashi, Y.Yoshino, and T.Ishiguro, "Effect of Stabilizing Treatment on Precipitation Behavior of Alloy 706", Superalloys 1996, ed., R.D.Kissinger et al. (Warrendale, PA:TMS, 1996), 627-636.
12. K.A.Heck, "The Time-Temperature-Transformation Behavior of Alloy 706", Superalloys 718, 625, 706 and Various Derivatives, ed., E.A.Loria (Warrandale, PA:TMS, 1994),, 393-404.
13. T.Shibata, Y.Shudo, and Y.Yoshino, "Effects of Aluminum, Titanium and Niobium on the Time - Temperature - Precipitation Behavior of Alloy 706", Superalloys 1996, ed., R.D.Kissinger et al. (Warrendale, PA:TMS, 1996) 153-162.
14. R.Cozar and A.Pineau, "Morphology of γ ' and γ " Precipitates and Thermal Stability of Inconel 718 Type Alloys", Metallurgical Transactions, 4(1973), 47-59.
15. J.P.Collier, S.H.Wong, J.C.Phillips, and J.K.Tien, "The Effect of Varying Al, Ti, and Nb Content on the Phase Stability of Inconel 718", ibid., 19A (1988), 1657-1666.
16. J.P.Collier, A.O.Selius, and J.K.Tien, "On Developing a Microstructurally and Thermally Stable Iron - Nickel Base Superalloy", Superalloys 1988, ed., D.N.Duhl et.al. (Warrendale, PA: The Metallurgical Society, 1988), 43-52.
17. E.Andrieu, R.Cozar, and A.Pineau, "Effect of Environment and Microstructure on the High Temperature Behav ior of Alloy 718", Superalloy 718 - Metallurgy and Applications, ed., E.A.Loria (Warrendale, PA:TMS, 1989), 241-256.
18. E.Gou, F.Xu, and E.A.Loria, "Effect of Heat Treatment and Compositional Modification on Strengthening and Thermal Stability of Alloy 718", Superalloys 718, 625 and Various Derivatives, ed., E.A.Loria (Warrendale, PA:TMS, 1991), 389-396.
19. E.Gou, F.Xu, and E.A.Loria, "Comparison of γ '/ γ " Precipitates and Mechanical Properties in Modified 718 Alloys", ibid., 397-408.
20. J.A.Manriquez, P.L.Bretz, L.R.Rabenberg, and J.K.Tien, "The High Temperature Stability of IN718 Derivative Alloys", Superalloys 1992, ed., S.D.Antolovich et al. (Warrendale, PA: TMS, 1992), 507-516.
21. E.Andrieu, N.Wang, R.Molins, and A.Pineau, "Influence of Compositional Modifications on Thermal Stability of Alloy 718", Superalloys 718, 625, 706 and Various Derivatives, ed., E.A.Loria (Warrendale, PA:TMS, 1994) 695-710.
22. X.Xie, Q.Liang, J.Dong, W.Meng, Z.Xu, M.Chen, F.Wang, Y.Cai, J.Zhang, N.Wang, E.Andrieu, and A.Pineau, "Investigation on High Thermal Stability and Creep Resistant Modified Inconel 718 with Combined Precipita tion of γ " and γ ' ", ibid., 711-720.
23. E.Gou, F.Xu, and E.A.Loria, "Further Studies on Thermal Stability of Modified 718 Alloys", ibid., 721-734.